

Validation Studies of Fluent

Turbulence Models for Fluent

Simulations of AguaClara Flocculators

AguaClara Computational Fluid Dynamics Spring 2010

Travis Stanislaus

1 Introduction:

The AguaClara water treatment project uses ANSYS Fluent computational fluid dynamics (CFD) software to simulate and analyze turbulent fluid flow in idealized models of flocculators in AguaClara water treatment plants. The flocculator simulations in Fluent are used to obtain turbulent kinetic energy dissipation rate, ϵ , and energy loss coefficient, K , between baffle in the flocculator for AguaClara design equations that determine the height of the flocculator, H , the spacing between baffles, S , the quantity of baffles in the flocculator, and flocculation performance, $\Theta\epsilon^{1/3}$, Θ is the residence time between two baffles. The results from Fluent are used in the design of AguaClara facilities, so verification and validation of the Fluent flocculator model and simulation has been conducted continuously since the time AguaClara began using Fluent simulations. Verification is determination of the degree the model being simulated is an accurate representation of the developer's description and solution to the model. Validation is determining if the model is an accurate representation of the real world physics and intended uses of the model.

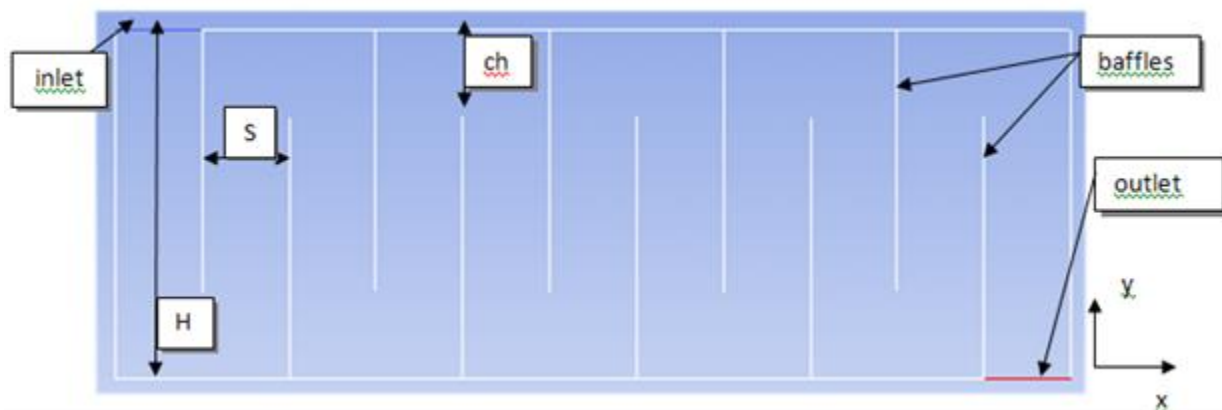


Figure 1: Fluent model of an AguaClara flocculator, where ch is the clearance height between the tip of a baffle and the top or bottom surface of the flocculator.

Each simulation of the flocculator in Fluent uses one of Fluent's turbulence models to approximate turbulence in the simulation because fluid flow in the real flocculator is turbulent and turbulence approximations allow the simulation to be completed in reasonable length of time of a few hours. Fluent simulations of flocculators of H/S ratios ranging from 4 to 40, using different turbulence models in Fluent, have never yielded $K < 3$ in the flocculator baffle spaces. Laboratory measurement of K in a specific H/S flocculator in Fall 2009 and Spring 2010 at Cornell University yielded an average of $K = 1.85$ in each baffle space. Measurement of K in the flocculator of the AguaClara facility in Agalteca, Honduras, in April 2010, yielded an average K of 1.96 in each baffle space. The flocculator in the AguaClara facility has a different H/S than the laboratory flocculator and these two measured K 's are significantly lower than the K 's obtained from Fluent simulations using Fluent turbulence models for the corresponding H/S flocculators. The contrast between K measured from physical flocculators and K obtained from Fluent led to new attempts to validate Fluent simulations of the Flocculator using the turbulence models available in the software package and assess the source of Fluent's error calculating K . The validation cases studied in Fluent were fluid flow geometries with known analytical solutions or documented experimental measurements.

2 Methods and Background:

Two dimensional geometries of the flocculator and two dimensional geometries for validation cases of Fluent simulations were created in the ANSYS design modeler and the geometries were discretized in the ANSYS mesher to create a mesh for simulation in Fluent. Pieces of the geometries were named in the mesher, such as, the inlet, outlet, walls, and baffles.

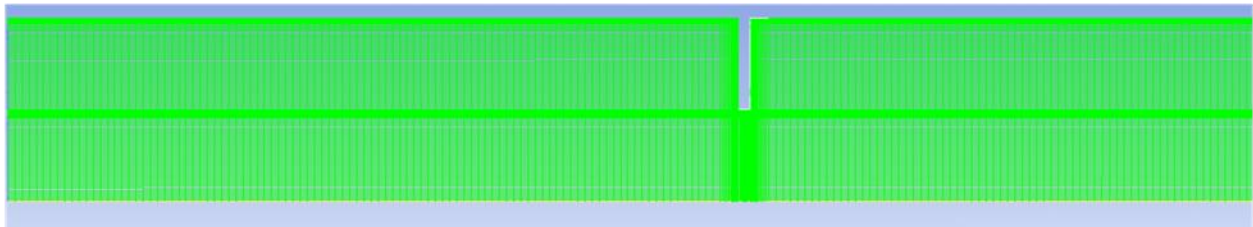


Figure 2: Mesh of a submerged orifice created in the ANSYS mesher.

The mesh was opened in ANSYS Fluent and the simulation was prepared. The conditions for the physics of simulation, the fluid material properties, turbulence model, and boundary conditions were set. The turbulence models available in Fluent are Spalart-Allmaras, $k-\epsilon$, $k-\omega$, Transition $k-\omega$, Transition SST, and Reynolds Stress. One turbulence model is used in a simulation. The simulation was

initialized and Fluent calculated a solution to 10^{-6} convergence.

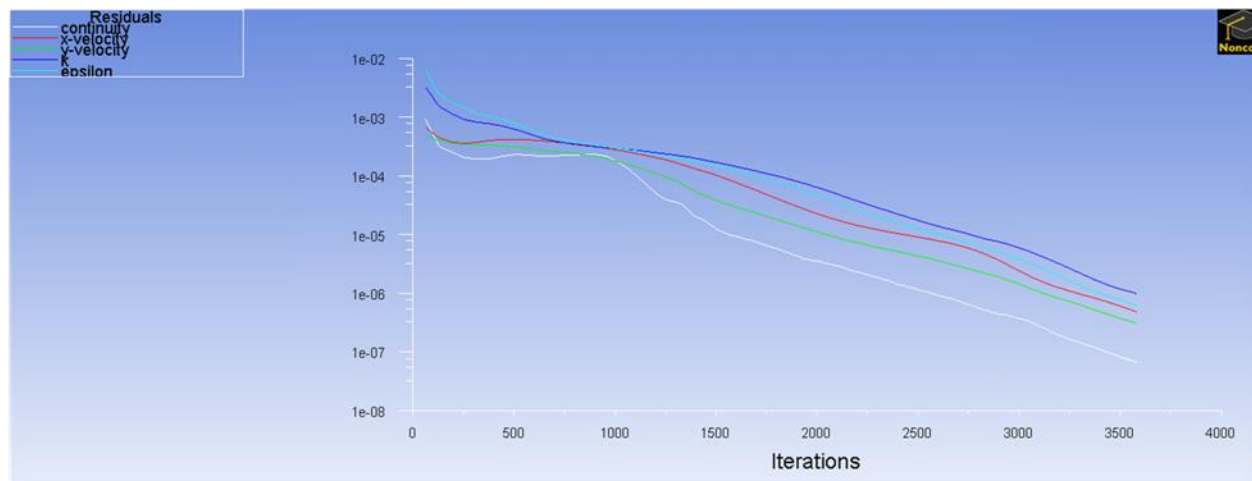


Figure 3: Iterative convergence in Fluent.

Grid convergence was used to determine if the number of nodes in the mesh affected the fluent solution.

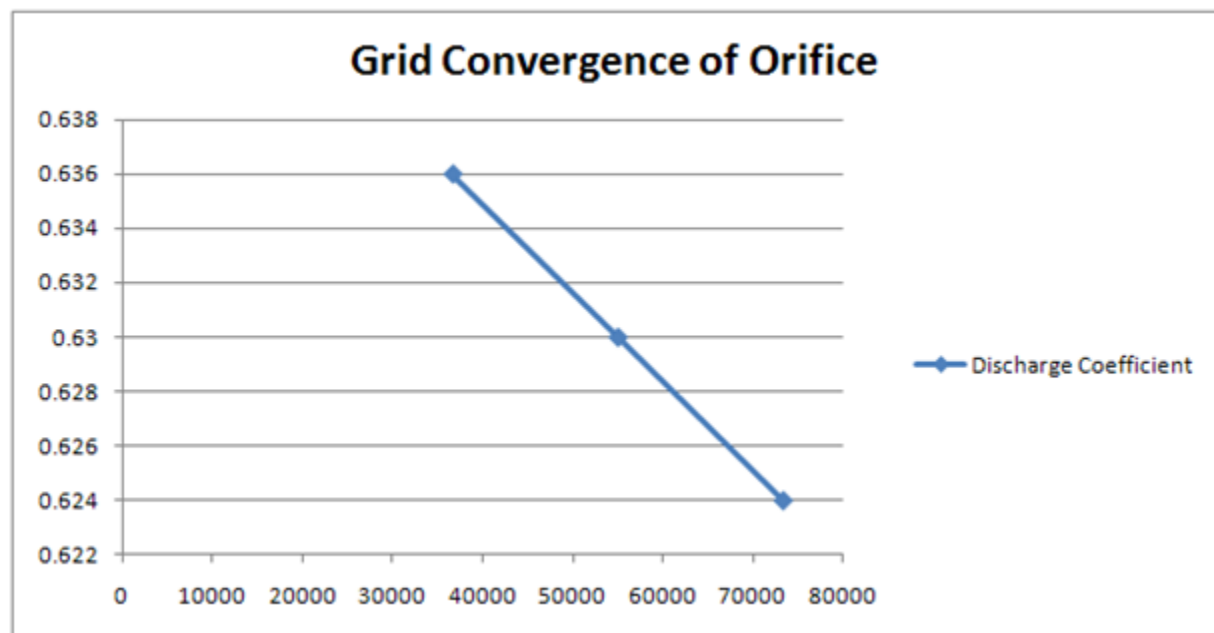


Figure 4: Effect of the number of nodes in the mesh on the discharge coefficient of an orifice simulation. As the number of nodes is increased, the simulation discharge coefficient approaches the reported discharge coefficient of 0.615 for Reynolds's Number (Re) = 18,400 in "Fluid Mechanics" by Frank White. The error of 73300 node mesh is 1.46%.

The simulation solution Y^+ at the walls of the geometry, shown in Figure 5, was checked to verify the turbulence model approximations of the turbulent boundary layer on the wall were correct.

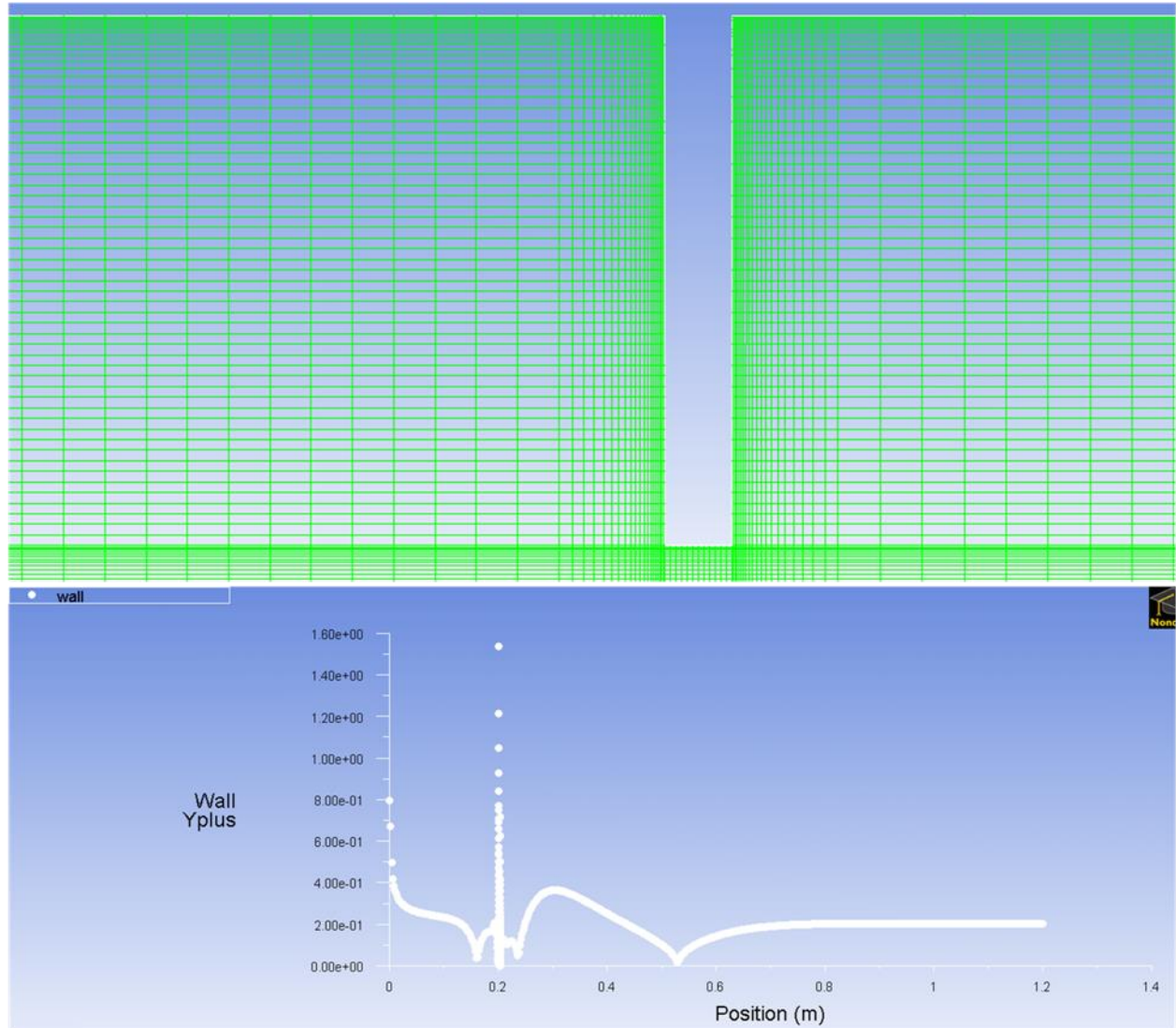


Figure 5: Refinement of mesh cells at the wall to achieve y^+ below 5.

The fluid flow in the flocculator was broken into simple fluid flow features to validate the Fluent simulation and investigate the location of Fluent's error calculating K. The flocculator has a contraction and an expansion at the recirculation zone after each turn and severe flow curvature around the end of the baffles. The validation cases assess Fluent's ability to correctly simulate fluid flow in these zones of the flocculator.

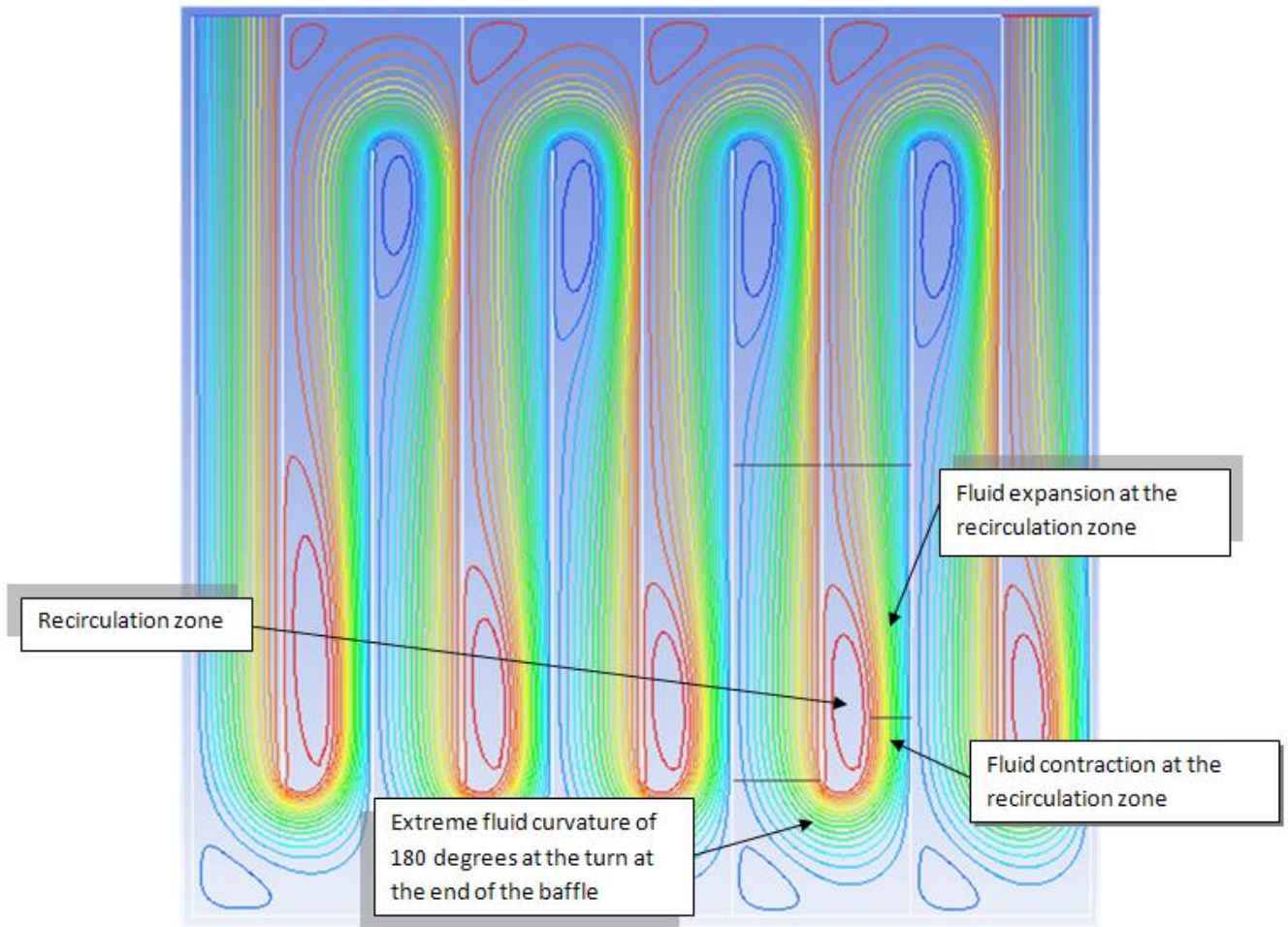
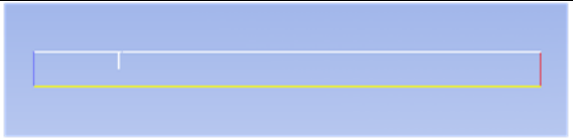



Figure 6: Flow features identified the flocculator with fluid flow visualized by streamlines. The line between the fluid contraction and expansion is one of the *vena contractas* of the fluid flow. $H/S = 10$.

Validation Cases		
Name	Region of Fluid Flow Examined	Geometry Configuration
(1) Discharge coefficient of a submerged orifice	Contraction of fluid flow in the flocculator	
(2) Energy loss coefficient between the inlet and outlet of fluid flow in a narrow pipe expanding into a wider pipe	Expansion of fluid flow in the flocculator	

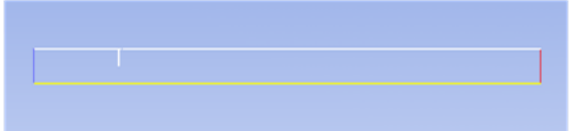
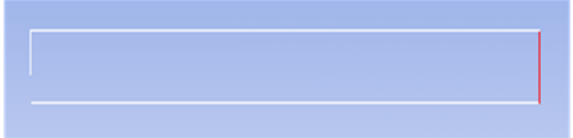
(3) Pressure recovery and velocity in a submerged orifice	Expansion of fluid flow immediately after fluid contraction	
(4) Comparison of K after the <i>vena contracta</i> of a submerged orifice and the flocculator (Each simulation inlet is the <i>vena contracta</i> of each geometry)	Difference between contraction of fluid flow and 180 degree curvature of fluid flow	

Table 1: Validation cases and corresponding region of fluid flow in the flocculator investigated.



Figure 7: Image of a full submerged orifice.

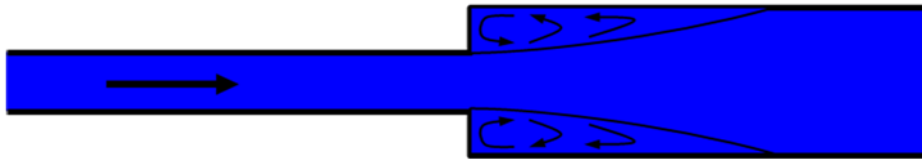


Figure 8: Full image of fluid flow from a narrow pipe expanding in a larger pipe.

Construction of the Validation Simulations	
1)	Planar simulation with centerline symmetry using the k- ϵ realizable model for $Re = 10000, 100000, 10000000$. Density, ρ , is 1000kg/m^3 and viscosity, ν , is $1 \times 10^{-3}\text{kg/m}\cdot\text{s}$. The inlet boundary conditions are inlet velocity $1\text{m/s}, 10\text{m/s}, 100\text{m/s}$, with turbulent intensity and hydraulic diameter 10% and 0.1m respectively. Pressure outlet with second order upwind settings for momentum, turbulent kinetic energy (k), and ϵ . The convergence criterion is 10^{-6} . The dimensions of the orifice are pipe diameter 0.1m , orifice diameter 0.06m , orifice width 3mm , length before orifice is 0.4m , and length after the orifice is 1m (the lengths before and after the orifice were increased for very large Re). The geometry built in the design modeler is half of the pipe because Fluent can simulate the pipe with symmetry along the middle of the pipe.
2)	Planar simulation with centerline symmetry using the k- ϵ realizable model for Reynolds Number (Re) = 10000 . Density, ρ , is 1000kg/m^3 and viscosity, ν , is $1 \times 10^{-3}\text{kg/m}\cdot\text{s}$. The inlet boundary condition is inlet velocity 1m/s with turbulent intensity and hydraulic diameter 10% and 0.2m respectively. Pressure outlet with second order upwind settings for momentum, turbulent kinetic energy (k), and ϵ . The convergence criterion is 10^{-6} . The pipe dimensions are small pipe diameter is 0.08m , large pipe diameter is 0.2m , length of the small pipe is 0.4m , and the length of the large pipe is 1m . The

<p>geometry built in the design modeler is half of the pipe because Fluent can simulate the pipe with symmetry along the middle of the pipe.</p>
<p>3) Axisymmetric simulation with the centerline of the pipe as an axis using the k-ε realizable model for one simulation and Reynolds stress model (RSM) for another simulation both at Re = 18400. Density, ρ, is 1000kg/m³ and viscosity, ν, is 1.003x10⁻³kg/m*s. The inlet boundary condition is inlet velocity 0.3m/s with turbulent intensity and hydraulic diameter 10% and 0.0615m respectively. Pressure outlet with second order upwind settings for momentum, k, and ε. The convergence criterion is 10⁻⁶. The dimensions of the orifice are pipe diameter 0.0615m, orifice diameter 0.03075m, orifice width 3mm, length before orifice is 0.2m, and length after the orifice is 1m. Half of the orifice is built in the design modeler because Fluent simulate half of the pipe as three dimensional with an axisymmetric simulation and setting the centerline of pipe as an axis.</p>
<p>4) Planar simulation using the k-ε realizable model with ρ = 1000kg/m³ and ν = 1x10⁻³kg/m*s. Two geometries for different simulations. One geometry has the flocculator <i>vena contracta</i> height of 0.045m as the inlet height and the inlet boundary conditions are the velocity, k, and ε profiles of the <i>vena contracta</i> in a flocculator simulation. The other geometry has the orifice <i>vena contracta</i> height of 0.038 m as the inlet height and the inlet boundary conditions are the velocity, k, and ε profiles of the <i>vena contracta</i> of a planar orifice simulation. Both geometries have length of 1m and outlet height = total height = 0.1m. Matlab code used to format the boundary condition profiles for input into Fluent is given in Appendix C.</p>

Table 2: Description of the settings of each simulation in Fluent.

2.I Discharge Coefficient of an Orifice:

The ratio of the orifice diameter, d, to the pipe diameter, D, is:

$$\beta = \frac{d}{D} \quad [1]$$

Analysis of the discharge coefficient in an orifice begins with the conservation of mass equation and Bernoulli's equation respectively:

$$Q = \rho_1 A_1 V_1 = \rho_2 A_2 V_2 \quad [2]$$

$$p_1 + \frac{1}{2}\rho V_1^2 + \rho_1 g z_1 = p_2 + \frac{1}{2}\rho V_2^2 + \rho_2 g z_2 \quad [3]$$

The density is constant and cancels out of the continuity equation. The continuity equation can be used to solve V₁ in terms of V₂ and Bernoulli's equation can be solved for V₂, leading to:

$$Q = V_2 A_2 = \left[\frac{2(p_1 - p_2)}{\rho \left(1 - \frac{A_2^2}{A_1^2}\right)} \right]^{1/2} \quad [4]$$

The discharge coefficient is a correction factor for using the orifice as flow measurement device by measuring the pressure difference at D before the orifice and $\frac{1}{2}D$ after the orifice to evaluate [4], but using the area of the orifice as A_2 in [4] since the area at $\frac{1}{2}D$ after the orifice is unknown. The discharge coefficient, C_d , can be solved from:

$$Q = A_1 V_1 = C_d A_{orifice} \left[\frac{2(p_1 - p_2)/\rho}{1 - \frac{A_{orifice}^2}{A_1^2}} \right]^{\frac{1}{2}} \quad [5]$$

2.II Energy Loss Coefficient:

The change in water level, head loss, h_L , is:

$$h_L = \frac{V_{ref}^2}{2g} K \quad [6]$$

K is the energy loss coefficient and an equation for h_L can be obtained from the pressures and velocities in a control volume by using the steady energy equation neglecting shear work:

$$(\dot{q}_{in} - \dot{w}_{shaft})\dot{m} = \int_{cs} \left(\frac{p}{\rho} + gz + \frac{V^2}{2} + \tilde{u} \right) \rho \mathbf{V} \cdot \mathbf{n} dA \quad [7]$$

The mass flux is:

$$\dot{m} = \int_{cs} \rho \mathbf{V} \cdot \mathbf{n} dA$$

And the energy equation assuming constant density becomes:

$$(\dot{q}_{in} - \dot{w}_{shaft})\dot{m} = \left[\left(\alpha_{p,out} \frac{p_{out}}{\rho} + gz_{out} + \alpha_{v,out} \frac{V_{out}^2}{2} + \tilde{u}_{out} \right) - \left(\alpha_{p,in} \frac{p_{in}}{\rho} + gz_{in} + \alpha_{v,in} \frac{V_{in}^2}{2} + \tilde{u}_{in} \right) \right] \dot{m} \quad [8]$$

Simplification of [8] and assuming no head loss due to pumps or turbines gives:

$$\alpha_{p,in} \frac{p_{in}}{\rho g} + z_{in} + \alpha_{v,in} \frac{V_{in}^2}{2g} = \alpha_{p,out} \frac{p_{out}}{\rho g} + z_{out} + \alpha_{v,out} \frac{V_{out}^2}{2g} + h_L \quad [9]$$

[9] solved in terms of h_L and assuming no elevation change in the control volume is:

$$h_L = \frac{\alpha_{p,in} p_{in} - \alpha_{p,out} p_{out}}{\rho g} + \frac{\alpha_{v,in} V_{in}^2 - \alpha_{v,out} V_{out}^2}{2g} \quad [10]$$

Substituting [10] in [6] and rearranging gives the energy loss coefficient based on pressure and velocity:

$$K = \frac{\alpha_{p,in}p_{in} - \alpha_{p,out}p_{out}}{\frac{1}{2}\rho V_{ref}^2} + \frac{\alpha_{v,in}V_{in}^2 - \alpha_{v,out}V_{out}^2}{V_{ref}^2} \quad [11]$$

α_v and α_p are energy correction terms to account for non-uniformity of the velocity or pressure profile in an area of geometry. Uniform pressure or velocity is $\alpha = 1$. Non-uniform profiles yield $\alpha > 1$. α is the non-uniform energy divided by what the uniform energy would have been, for example, differing profiles of kinetic energy and pressure of the energy equation:

$$\int_{cs} \left(\frac{V^2}{2} \right) \rho \mathbf{V} \cdot \mathbf{n} dA = \alpha_v \frac{\rho \bar{V}^3 A}{2}$$

$$\alpha_v = \frac{1}{A} \int_{cs} \left(\frac{V^2}{\bar{V}^3} \right) \mathbf{V} \cdot \mathbf{n} dA$$

$$\int_{cs} P \mathbf{V} \cdot \mathbf{n} dA = \alpha_p \bar{P} \bar{V} A$$

$$\alpha_p = \frac{1}{A} \int_{cs} \frac{P \mathbf{V} \cdot \mathbf{n}}{\bar{P} \bar{V}} dA$$

\bar{V} is the average normal velocity on a control surface and \bar{P} is the average normal pressure.

V is the point velocity, P is the point pressure, and $\mathbf{V} \cdot \mathbf{n}$ is the normal velocity.

Analytical approximations for K can be obtained using the conservation of mass, momentum, and energy equations, respectively, on a control volume:

$$\rho_{in} A_{in} V_{in} = \rho_{out} A_{out} V_{out}$$

$$p_{in} A_{in} + \rho_{in} V_{in}^2 A_{in} = p_{out} A_{out} + \rho_{out} V_{out}^2 A_{out} \quad [12]$$

$$h_L = \frac{p_{in} - p_{out}}{\rho g} + \frac{V_{in}^2 - V_{out}^2}{2g}$$

Density is assumed constant and conservation of mass becomes:

$$\frac{A_{in}}{A_{out}} = \frac{V_{out}}{V_{in}} \quad [13]$$

Density is assumed constant for the momentum equation and the assumption to obtain the analytical approximations of K is, divide [12] by A_{out} and assume A_{in}/A_{out} on the p_{in} term is 1. This assumes that P_{in} is uniformly distributed on the control volume surface of the inlet that is equal to the outlet control volume surface when in fact the pressure varies on the inlet control surface, such as in Figure9, where

there is an expanding fluid jet and a recirculation zone on the inlet of the control volume. The differences in area on the velocity terms are maintained. The momentum equation with the assumption is:

$$p_{in} - p_{out} = \rho \left(V_{out}^2 - V_{in}^2 \frac{A_{in}}{A_{out}} \right) \quad [14]$$

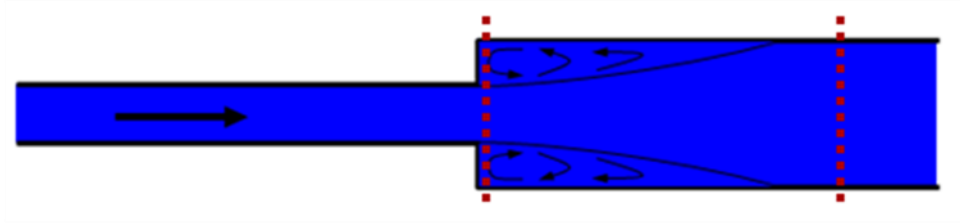


Figure 9: Fluid flow expanding from a small pipe in a large pipe with a control volume denoted by the dotted lines used to derive the analytical approximations of K.

Dividing both sides by ρ and g gives:

$$\frac{p_{in} - p_{out}}{\rho g} = \frac{V_{out}^2 - V_{in}^2 \frac{A_{in}}{A_{out}}}{g} \quad [15]$$

[15] can be inserted into [10], assuming all α 's = 1, and give h_L in terms of only velocity and area. Then [13] can be inserted into [10] to give h_L in terms of velocity:

$$h_L = \frac{V_{out}^2 - V_{in}^2 \frac{A_{in}}{A_{out}}}{g} + \frac{V_{in}^2 - V_{out}^2}{2g} \quad [16]$$

[16] can be simplified to obtain:

$$h_L = \frac{(V_{in} - V_{out})^2}{2g} \quad [17]$$

And using [13] h_L can be written as:

$$h_L = \frac{V_{in}^2}{2g} \left[1 - \frac{A_{in}}{A_{out}} \right]^2 = \frac{V_{out}^2}{2g} \left[\frac{A_{out}}{A_{in}} - 1 \right]^2 \quad [18,19]$$

[18] and [19] follow the form of [6], so the analytical approximations for K are:

$$K_{expansion} = \left[1 - \frac{A_{in}}{A_{out}} \right]^2 \quad [20]$$

$$K_{pressure} = \left[\frac{A_{out}}{A_{in}} - 1 \right]^2 \quad [21]$$

[18] has $K_{expansion}$ because the head loss is based on the inlet velocity. The inlet velocity travels through a smaller area than the outlet velocity so the inlet velocity must be greater. The fluid slows down from the inlet to the outlet because of energy loss from fluid expansion and $K_{expansion}$ represents the energy loss from the fluid slowing down. [19] has $K_{pressure}$ because the head loss in [19] is based on the outlet velocity and depends on how the energy is lost before the outlet.

3 Results:

The results of the simulation of Validation case 1 in table using an orifice with $\beta = 0.6$ are given in Table 3.

1) Discharge Coefficient of Orifice		
Re	C_d calculated from Fluent	C_d from "Fluid Mechanics", [E]
10^4	0.6285	0.633
10^5	0.6087	0.611
10^6	0.606	0.6

Table 3: Discharge coefficients from Fluent simulation and measurements.

The results validation case 2 analyzing K are given in Table 4.

2) Analysis of K for a small pipe expanding into a large pipe.			
Re	D_{in}/D_{out}	$K_{expansion}$	K calculated from Fluent simulation
10^4	0.4	0.36	0.2976

Table 4: Analytical $K_{expansion}$ and K from Fluent simulation.

Validation case 3 compared pressure recovery in an orifice in a Fluent simulation using k- ϵ realizable and RSM turbulence models with dimensionless pressure recovery and centerline velocity distribution plots from orifice experimental measurements in the dissertation, "A Study of 3-Dimensional Flow Through Orifice Meters", [A]. The comparisons between Fluent and the orifice experiment were compared with

results from “Numerical Investigation of Turbulent Flow through a Circular Orifice”, [B], which compared the same orifice experimental data with CFD k- ϵ and RSM turbulence model simulations.

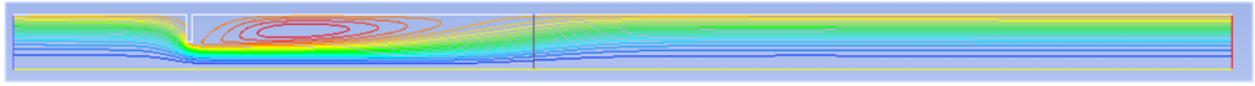


Figure 10: Streamlines for k- ϵ realizable simulation of the orifice with reattachment at 0.2m from the orifice or $x/R= 9.76$.

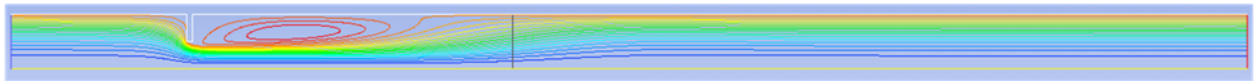


Figure 11: Streamlines for RSM simulation of the orifice with reattachment at 0.185m from the orifice or $x/R= 9.26$.

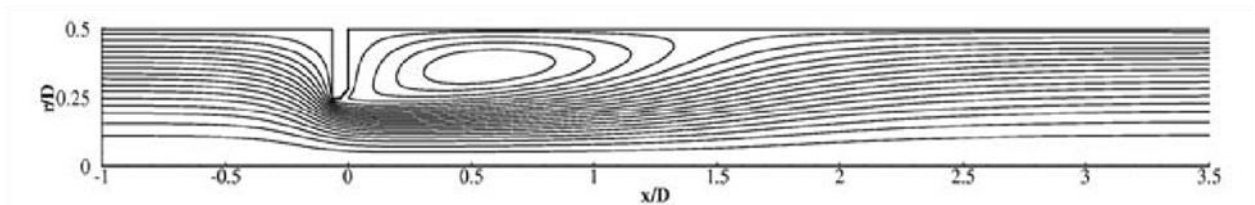


Figure 5 Streamlines predicted by the k- ϵ model.

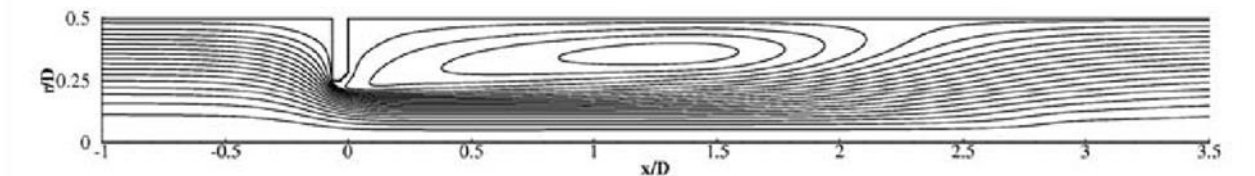


Figure 6 Streamlines predicted by the RSM.

Figure 12: Streamlines for k- ϵ and RSM turbulence models in “Numerical Investigation of Turbulent Flow through a Circular Orifice”, [B].

The reattachment length of the experiment is 0.13161m from the orifice.

Orifice wall-static pressure

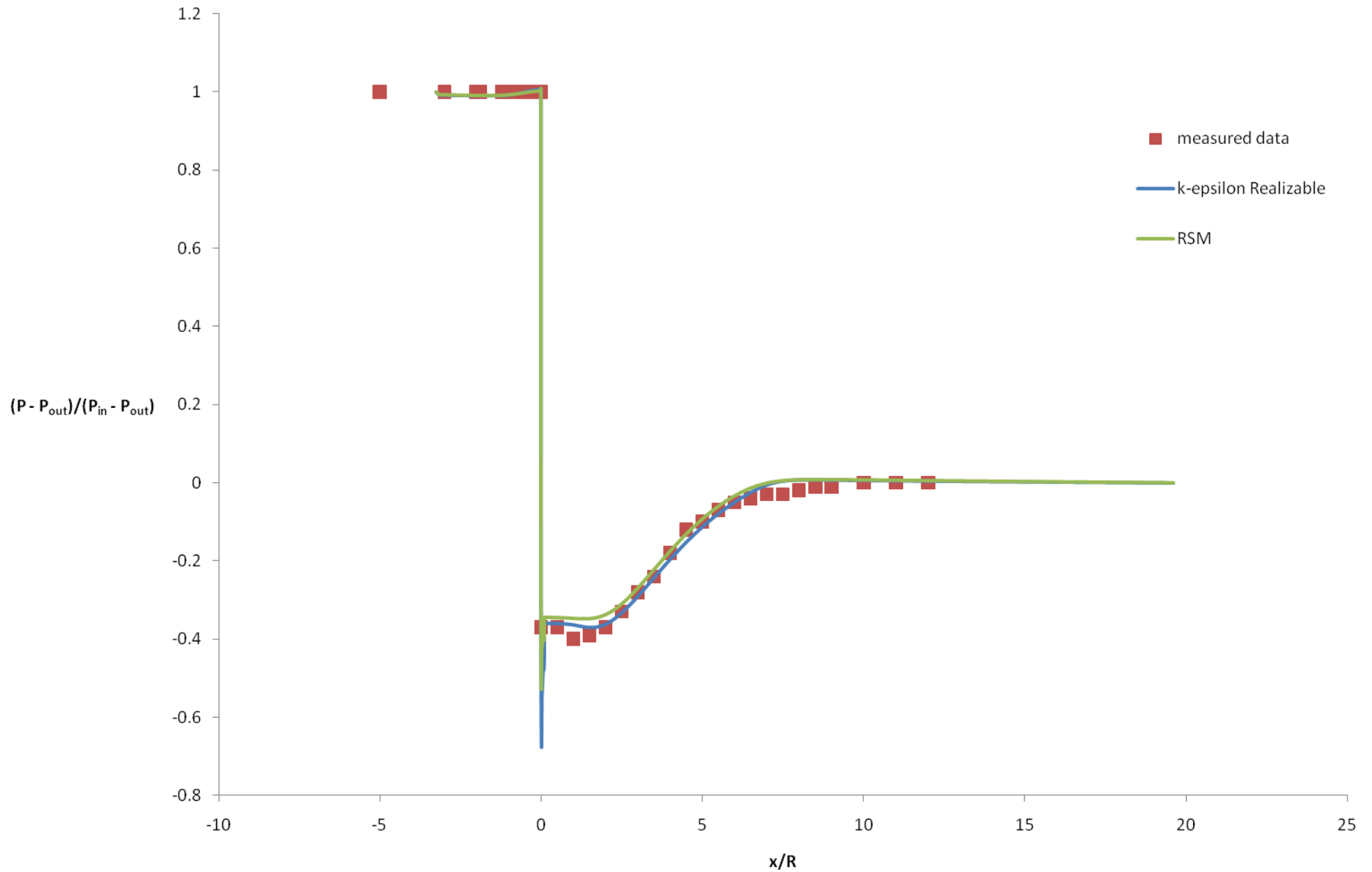


Figure 13: Dimensionless pressure recovery in orifice simulated in fluent and experimental measurements.

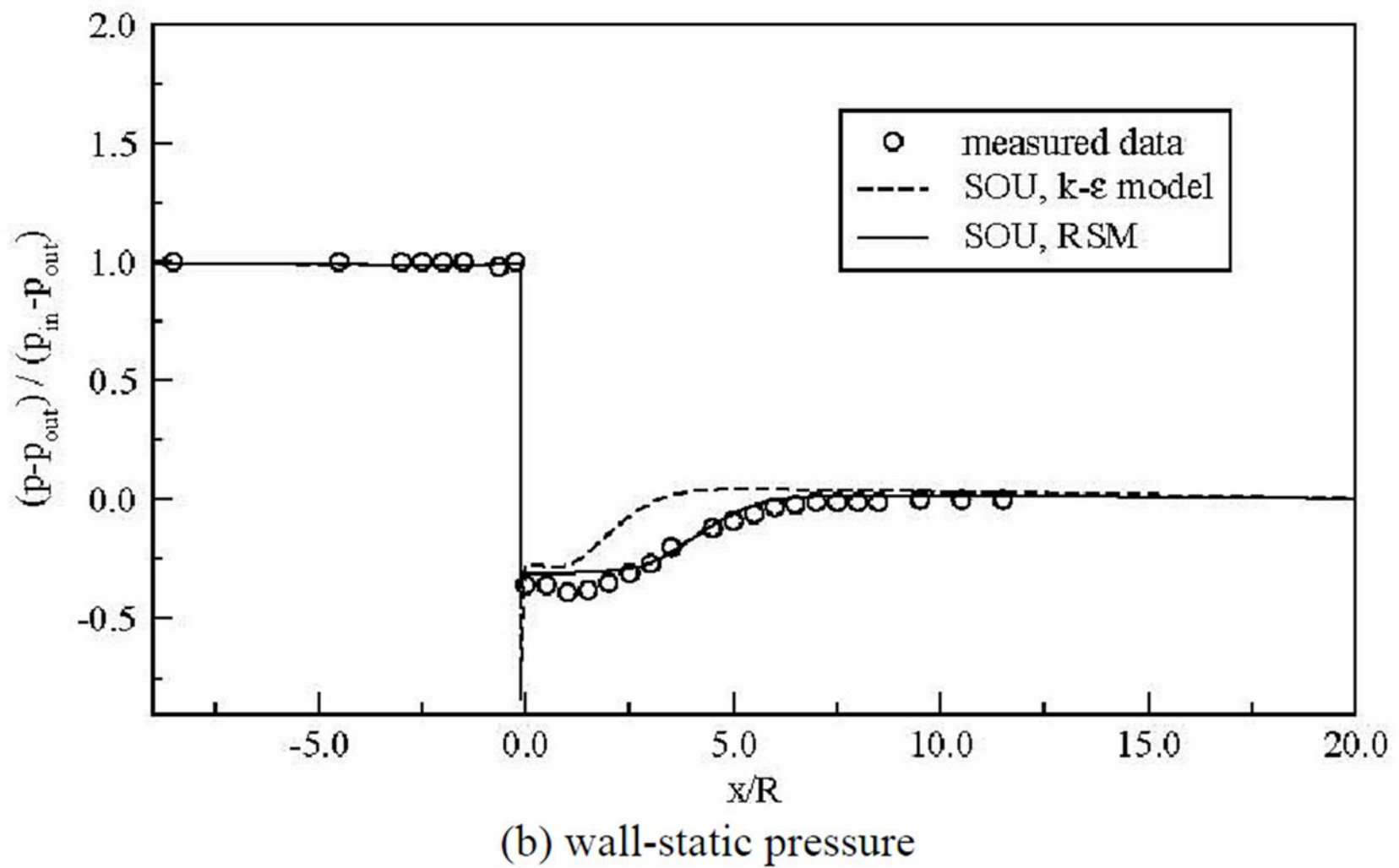


Figure 14: Dimensionless pressure comparison between CFD and experimental measurements in “Numerical Investigation of Turbulent Flow through a Circular Orifice”, [B].

Centerline axial velocity

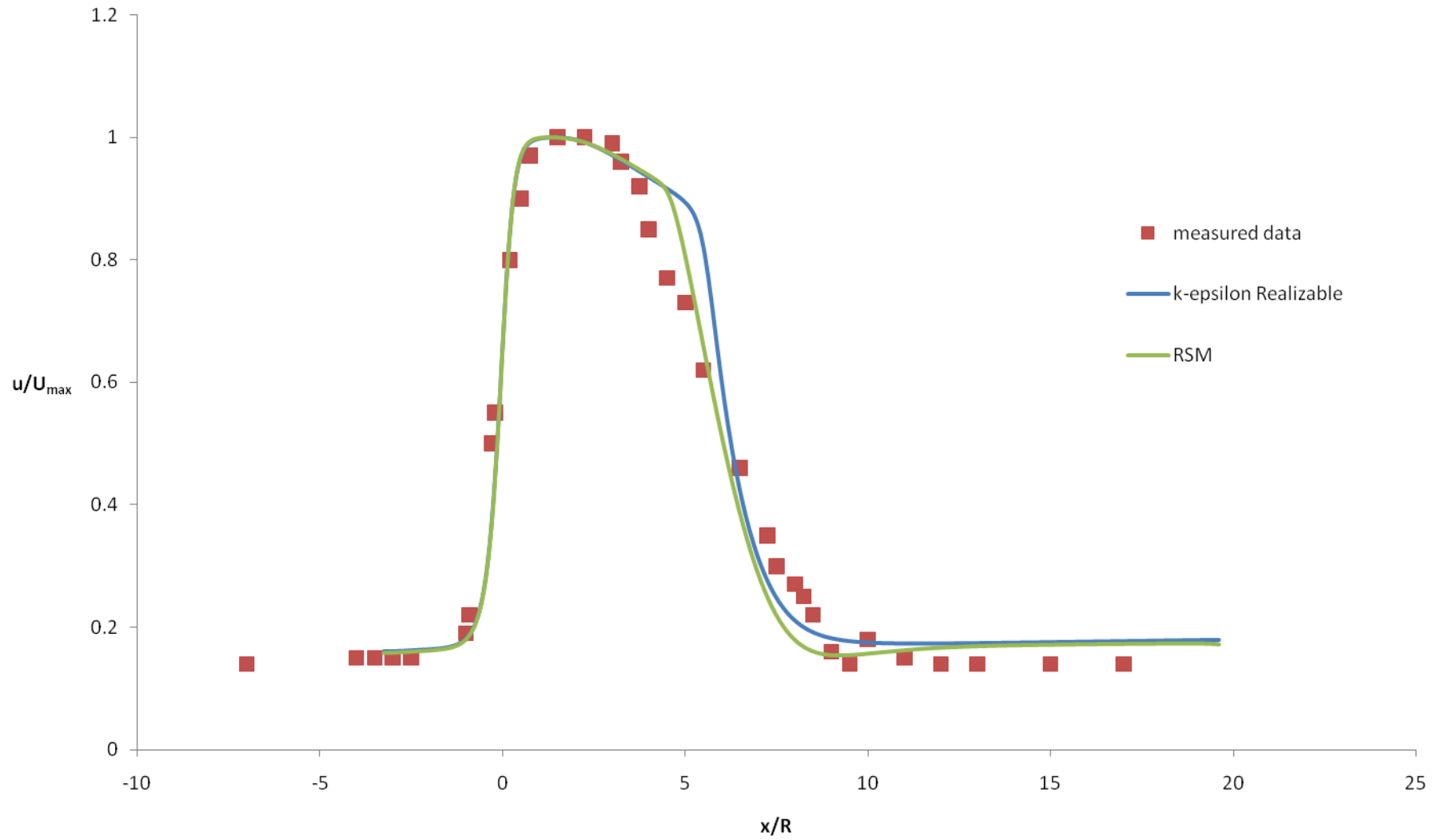
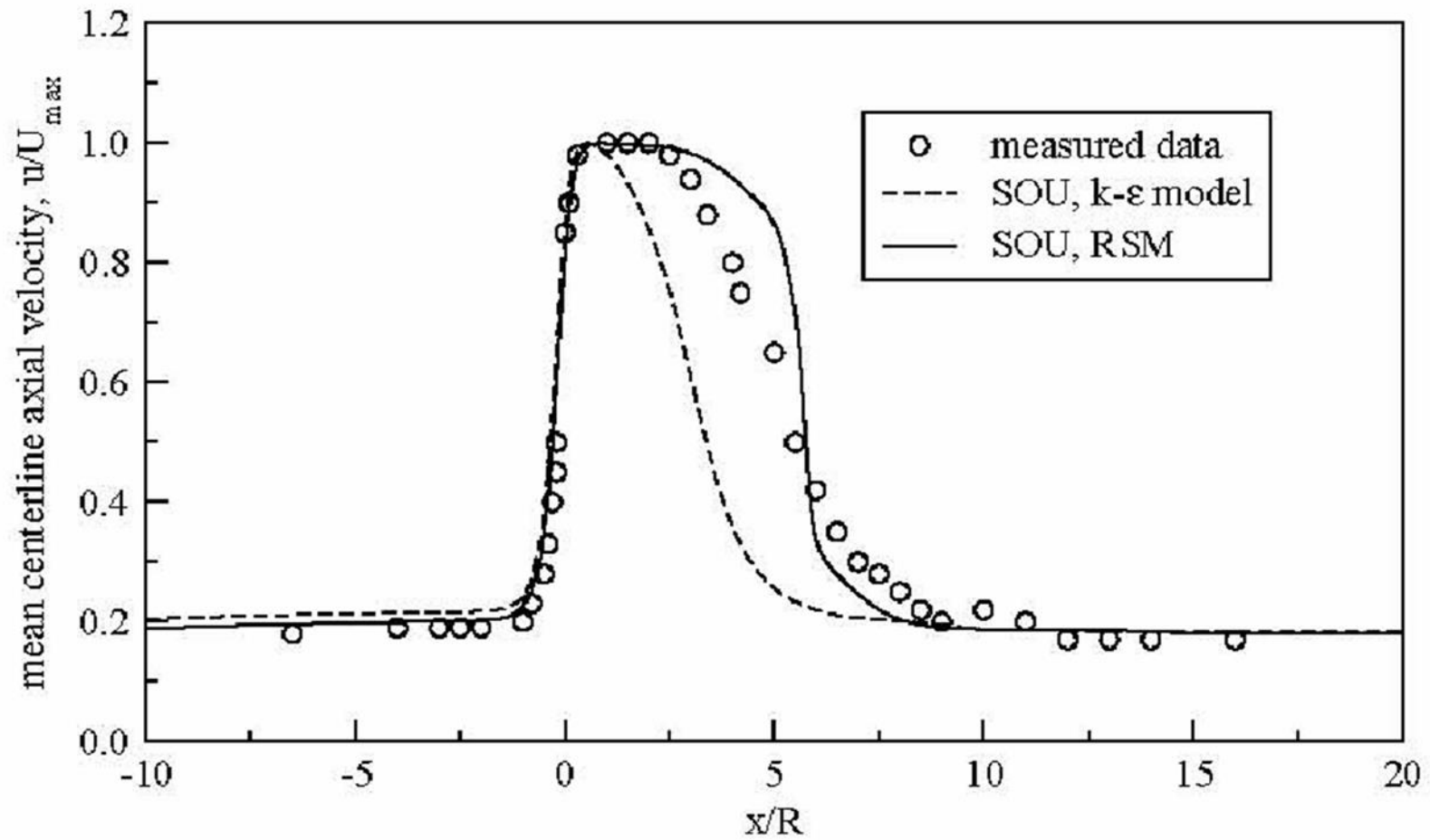


Figure 15: Dimensionless centerline velocity from orifice simulated in Fluent compared with orifice experimental measurements.



(a) centerline axial velocity

Figure 16: Dimensionless centerline velocity comparison between CFD and experimental measurements in “Numerical Investigation of Turbulent Flow through a Circular Orifice”, [B].

The K values from validation case 4 comparing the *vena contractas* of the orifice and flocculator are given in Table 4.

4) K in the <i>vena contracta</i> of the flocculator and orifice		
	K from Fluent	Analytical K_{pressure} , A_{in} is <i>vena contracta</i> area
Flocculator <i>vena contracta</i>	1.67	1.49
Orifice <i>vena contracta</i>	3.16	2.66

Table 5: Analytical K_{pressure} and K from Fluent simulation.

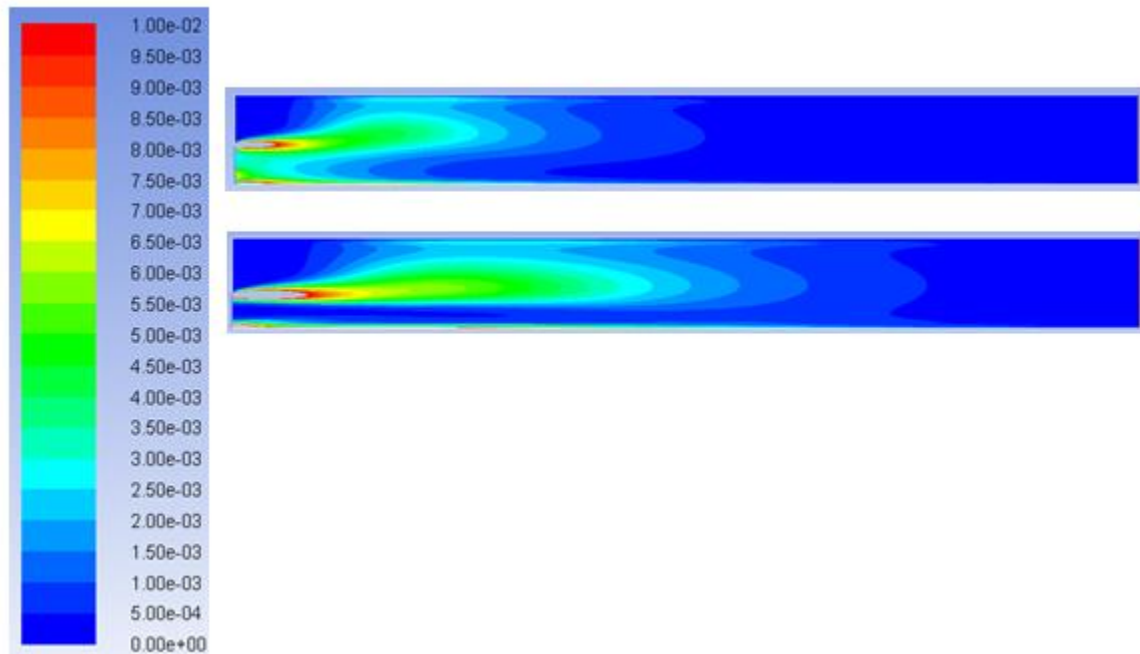


Figure 17: Contours of ε in the flocculator vena contracta simulation (top) and orifice vena contracta simulation (bottom) with the same scale.

Planar, 2D simulations of an orifice with $Re = 10000$, $\beta = 0.5$, $D = 0.1$ m, $L_{\text{total}} = 1$ m, and $V_{\text{in}} = 0.1$ m/s, and a flocculator with $Re = 10000$ $H/S = 10$, $S = 0.1$ m, and $V_{\text{in}} = 0.1$ m/s, both using the k - ε realizable turbulence model were run in Fluent to assess K, [11], in sections of the flocculator and orifice shown in Figure 18.

K in sections of the flocculator and orifice						
	$K_{1,2}$	$K_{2,3}$	$K_{3,4}$	$K_{4,5}$	$K_{5,6}$	Sum of K
Flocculator	0.087	-5.503	7.356	1.32	None	3.264
Orifice	-.911	-6973.3	6975.31	2.2	0.52	3.83

Table 6: Values of K in sections of the flocculator and orifice simulated in Fluent.

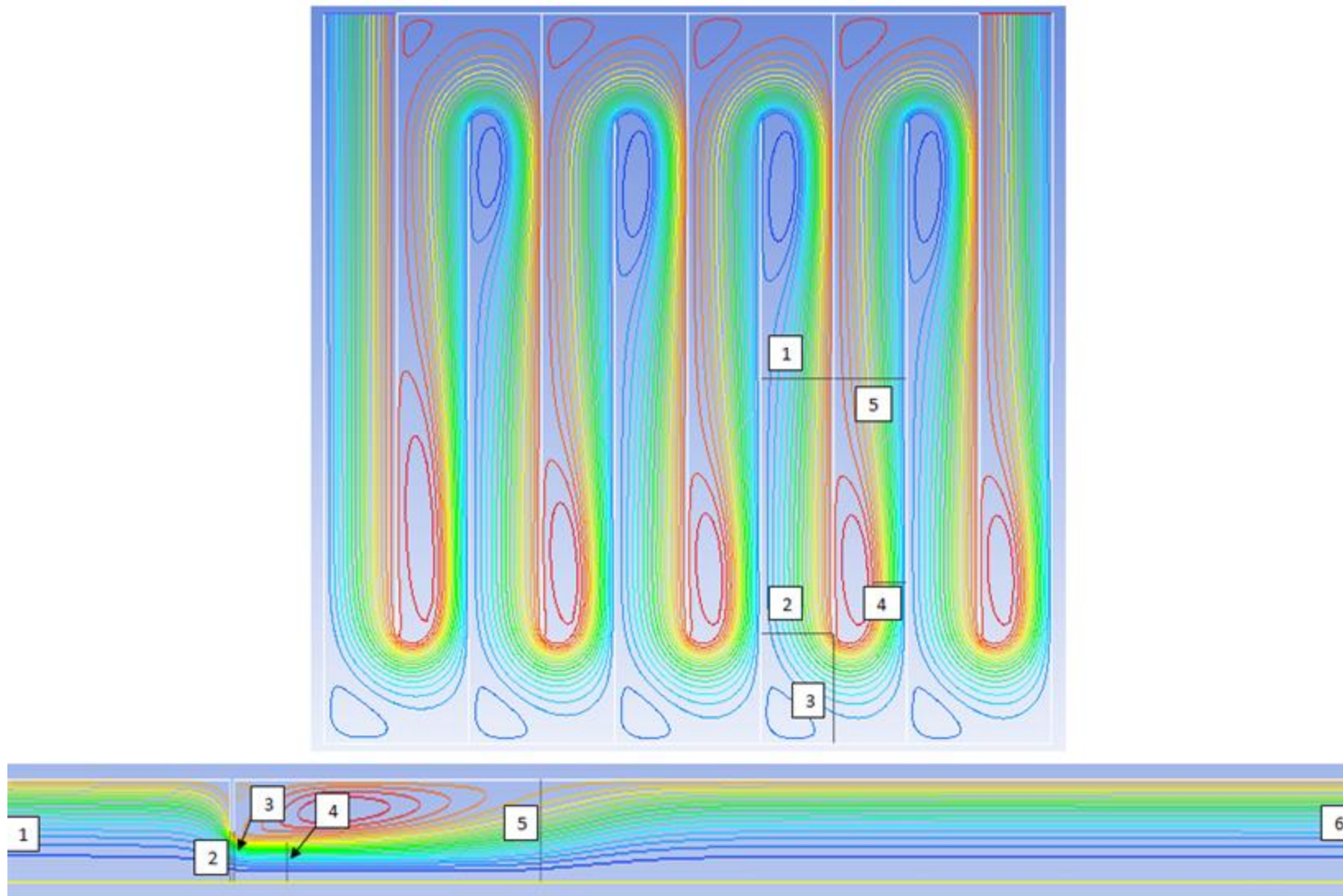


Figure 18: Sections of the flocculator (top picture) and orifice (bottom picture).

4 Discussion:

Validation case 1 was used to test Fluent's ability to correctly calculate fluid flow in a contraction and Fluent's C_d matches measured C_d well in Table 3. The K 's in the expanding pipes in validation case 2 in Table 4 do not match as well as validation case 1, however, it is difficult to assess the correctness of Fluent with this K because it is only compared to $K_{\text{expansion}}$ which is an approximation. Validation case 3 assesses the pressure recovery in a Fluent simulation and determines if the features of the flow in Fluent match reality.

Figures 13 and 15, and 14 and 16 demonstrate the Fluent comparison with experimental orifice measurements matches the CFD comparison with experimental orifice measurements in "Numerical Investigation of Turbulent Flow through a Circular Orifice", [B]. Figure 13 and Figure 15 show the dimensionless profile of pressure and velocity of the orifice calculated in Fluent match the experimental orifice of corresponding Re well. These figures withhold whether the point values of pressure and velocity match for the orifice simulated in Fluent and experimental orifice. At the orifice at $x/R = 0$ in Figure 13, the $k-\epsilon$ realizable model calculates a greater pressure difference than RSM and both models calculate greater pressure differences at the orifice than exist in the experiment. In the pressure recovery zone immediately following the orifice, $k-\epsilon$ realizable and RSM fit the experimental pressure recovery, however, $k-\epsilon$ realizable recovers pressure slightly faster than RSM. This subtle difference could relate to characteristic of $k-\epsilon$ realizable calculating a higher K in the flocculator than RSM.

In Figure 15, both turbulence models overestimate the velocity of the fluid after the orifice, have a faster decline of velocity than the experiment, and calculate higher velocity than the experiment when the velocity stabilizes after the orifice. Figure 15 also shows $k-\epsilon$ realizable overestimates the velocity after the orifice more than RSM and predicts a steeper decline in fluid velocity. The turbulence models calculate the velocities in the fluid expansion zone of the submerged orifice incorrectly. The recirculation zones in the Fluent simulation of the orifice are greater than the recirculation zone measured in the orifice experiment. The flocculator has a fluid expansion region and recirculation region too, which the turbulence models may incorrectly calculate as well. If the recirculation region is calculated incorrectly, the velocities in the simulation will be wrong in those sections. The potential mistake in velocity calculation in flocculator simulations holds with the observation that a Fluent flocculator simulation given a known head loss across the number baffles in the simulation reported a fluid velocity resulting in $K > 3$ as well.

Validation case 4 shows how K in the *vena contracta* of the flocculator and orifice differ, but similar to validation case 2, it is difficult to assess the correctness of the *vena contracta* K 's in Table 5 because they are compared to the approximation K_{pressure} . Figure 17 shows the difference between ϵ in the *vena contracta* of the orifice and flocculator. The orifice has ϵ concentrated at the edges of the *vena contracta* and the flocculator has ϵ throughout the *vena contracta*. The orifice appears to have a symmetric ϵ at the *vena contracta* and the flocculator has non-symmetric ϵ at the *vena contracta*. The 180 degree bend in the flocculator may cause the non-symmetric profile of ϵ in the *vena contracta*.

The K in sections of the flocculator and orifice in Table 6 and Figure 18 sum to K reported by their respective Fluent plot and show the deficiency in using K derived in [11] analyzing for turbulent flow. [11] addresses non-uniform velocity and pressure at different points in a flow because the α 's are integrated and use the mean velocity. This is only the time-averaged velocity in a turbulent flow and the velocity fluctuations, or instantaneous turbulent velocity profile, is not included in [11]. Velocity fluctuations give k, and the K's in different sections of the flocculator and orifice do not include k, therefore, cannot show how K is distributed throughout the orifice and flocculator. For example, $K_{2,3}$ and $K_{3,4}$ from the flocculator cannot be used to show Fluent's prediction of K in the turn of the flocculator and assess how fluid flow in that section contributes to Fluent's prediction of $K > 3$ between two baffles. The C_d assumes no energy is lost until the *vena contracta* of the orifice because the C_d analysis uses Bernoulli's equation. The flocculator has a *vena contracta* as well and analyzing K in sections before the flocculator and orifice *vena contractas* would show if they behave similarly. The velocities in the energy equation, [7], and energy correction factors, α_v and α_p , must be time averaged to include k. The velocity time average is:

$$V = \bar{V} + V' \quad [22]$$

\bar{V} is the mean velocity and V' is the velocity fluctuation.

The K values calculated from Fluent in validation cases 2 and 4 cannot be used to assess the flocculator simulation because K was calculated without k.

Interesting measurements of pressure drop across an orifice were found in "Measurement of Gas and Liquids by Orifice Meter", [D]. For a $\beta = 0.5$ orifice, $K_{\text{measurement}}$, [11], is 31.04 and it is independent of Re. For circular pipe, A in [21] is the area of a circle and A_{in} is orifice *vena contracta* area and A_{out} is the pipe area. The diameter of the orifice *vena contracta* is 38% of the pipe diameter. $K_{\text{pressure}} = 35.11$. Using k- ϵ realizable, $K = 27.76$ and $C_d = 0.63$ for $Re = 10,000$. $C_d = 0.62$ for $\beta = 0.5$ orifice at $Re = 10,000$ in "Fluid Mechanics" by Frank White. $K = 29.29$ with the RSM. Fluent calculates C_d well, however, Fluent calculates K incorrectly for the orifice. This matches Fluent's incorrect calculation of K in the flocculator, but Fluent under-predicts K in the orifice and over-predicts K in the flocculator.

5 Conclusion:

The validation cases show Fluent simulations, using the k- ϵ realizable and RSM turbulence models, do not completely match real world physics. Also the validation cases cannot specifically show the features of the turbulence models that cause the Fluent simulations to deviate from reality. Fluent is useful for obtaining accurate calculation of some fluid flow parameters, such as C_d of an orifice and process of Fluent simulation may simply be to figure out which fluid flow geometries and parameters Fluent calculates correctly and not use Fluent for anything else. The incorrect value of K from Fluent simulations using the turbulence models may be an inherent error from the turbulence approximation since Fluent incorrectly calculates K for the orifice and the flocculator. Large eddy simulation or direct numerical simulation of the flocculator may yield a correct K since the turbulent fluctuations are

calculated and stored. K in the orifice Fluent simulation is lower than measured K and the reattachment length is longer than the reattachment length of the experimental orifice, the longer reattachment length is reason the Fluent centerline velocities are over-predicted in Figure 15. The reattachment length in the Fluent flocculator simulation may be smaller than the reattachment length in the physical flocculator because the Fluent simulation K is higher than measured K , however there is no measurement of the reattachment length in physical AguaClara flocculators. Turbulent kinetic energy in the k - ϵ realizable model is calculated with the transport equation, [23] in Appendix B, and the generation of k is given by [24] and is directly proportional to velocity gradients. Figure 20 shows the velocity gradients of the flocculator and orifice. The generation of k model proportional to velocity gradients in k - ϵ realizable may contribute to Fluent's high K in the flocculator. The validation cases result in Fluent turbulence models not being suitable to produce a correct simulation of the flocculator. A turbulent simulation without as many turbulence approximations and modeling as the Fluent turbulence models may generate accurate flocculator simulations that can contribute correctly to AguaClara flocculator design.

References:

- [A] G.H. Nail. A Study of 3-Dimensional Flow Through Orifice Meters. Dissertation Texas A&M University.
- [B] S. Eiamsa-ard, A. Ridluan, P. Somravysin, and P. Promvonge. Numerical Investigation of Turbulent Flow through a Circular Orifice. KMITL Sci. J. Vol.8 No.1 January – June, 2008.
- [C] Guide for the Verification and Validation of Computational Fluid Dynamics Simulations. American Institute of Aeronautics and Astronautics.
- [D] H.P. Westcott and J. Christopher Diehl. Measurement of Gas and Liquids by Orifice Meter. Metric Metal Work, Second Edition, 1922.
- [E] F. M. White. Fluid Mechanics. McGraw Hill, Sixth Edition.
- [F] M. Weber-Shirk. Flocculation. <https://confluence.cornell.edu/display/cee4540/Syllabus>
- [G] M. Weber-Shirk. Finite Control Volume Analysis. <http://ceeserver.cee.cornell.edu/mw24/cee331/>

Appendix A:

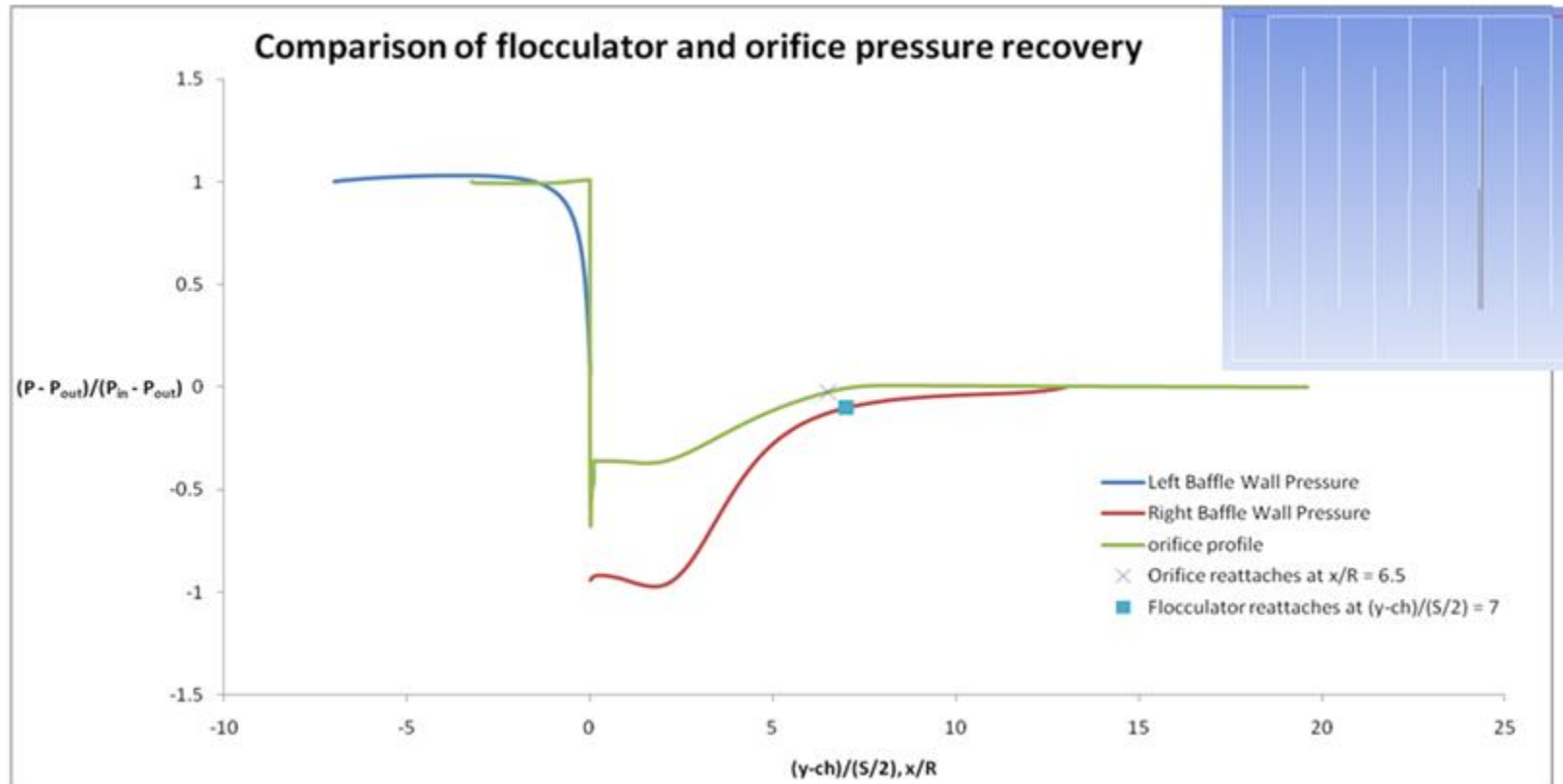


Figure 19: Dimensionless press in the flocculator and orifice simulation (wall pressure of the orifice is measured on the left line in the flocculator then the right line on the opposite wall after the turn). $0.15m \leq y \leq 0.5m$ on the left line and $0.15m \leq y \leq 0.8m$ on the right line. $ch = 0.15$ m. The flocculator continuously recovers pressure after the turn, while the orifice stops recovering pressure soon after reattachment.

Appendix B:

Velocity gradients in k-ε realizable simulation and generation of k in k-ε realizable turbulence model

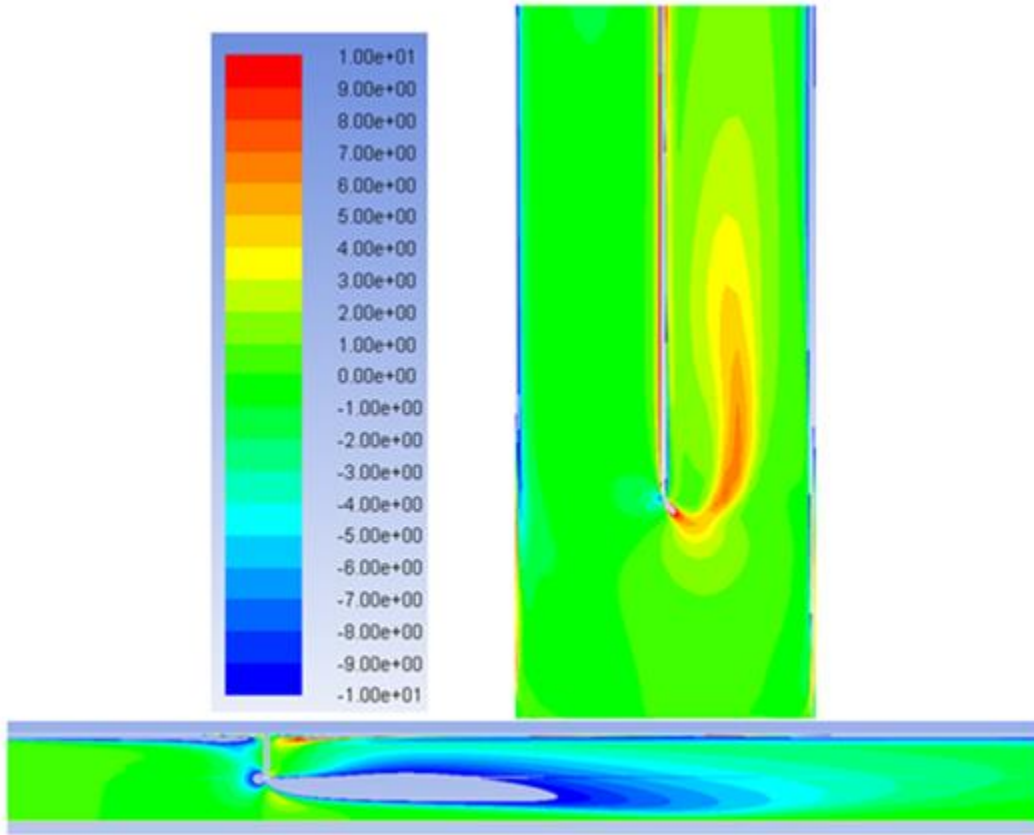


Figure 20: Velocity derivatives from Fluent in the k-ε simulation, the flocculator is dy/dx and the orifice is dx/dy . Velocity gradients are very high at the walls and may cause k to be calculated incorrectly in simulations with the k-ε realizable turbulence model.

Turbulent kinetic energy in the k-ε turbulence model is approximated by:

$$\frac{\partial}{\partial t}(\rho k) + \frac{\partial}{\partial x_j}(\rho k u_j) = \frac{\partial}{\partial x_j} \left[\left(\mu + \frac{\mu_t}{\sigma_k} \right) \frac{\partial k}{\partial x_j} \right] + G_k + G_b - \rho \epsilon - Y_M + S_k \quad [23]$$

And G_k is the production of k , which is proportional to the velocity gradient:

$$G_k = -\rho \overline{u'_i u'_j} \frac{\partial u_j}{\partial u_i} \quad [24]$$

Appendix C:

Matlab code modified from Matlab code provided by Dr. Rajesh Bhaskaran.

```
%Boundary profiles of turbulence quantities at the inlet  
%Taken from Jovic and Driver (1994)
```

```
%Output profiles:
```

```
N_out = 43;  
x_h_out = linspace(0,0,N_out);  
y_h_out = linspace(0,.045,N_out);  
U_out = [0  
0.0422303  
0.0895736  
0.136069  
0.174423  
0.20236  
0.221673  
0.234336  
0.242056  
0.246377  
0.248467  
0.249074  
0.248887  
0.248361  
0.247472  
0.246143  
0.245071  
0.243929  
0.242719  
0.241446  
0.240109  
0.238707  
0.237237  
0.235695  
0.234072  
0.232361  
0.230548  
0.228622  
0.226564  
0.224352  
0.221957  
0.219343  
0.21646  
0.213241  
0.209596  
0.205397  
0.200466  
0.194554  
0.187328  
0.178399  
0.167445  
0.154434  
0.150768  
];
```

```
tke_out = [1.63E-05
8.02E-05
0.000310458
0.000648818
0.000894497
0.000986665
0.00104019
0.00113903
0.00131109
0.00155054
0.00183815
0.00211536
0.00230329
0.00243119
0.002568
0.0027103
0.00279642
0.00286947
0.00293123
0.00298292
0.00302552
0.00305987
0.0030867
0.00310669
0.00312047
0.00312863
0.00313177
0.00313048
0.00312539
0.00311726
0.00310695
0.00309553
0.0030842
0.00307446
0.0030682
0.0030678
0.00307618
0.00309654
0.00313151
0.00318087
0.00323675
0.00328001
0.00328101
];
```

```
eps_out = [0.00801484
0.00933891
0.0122333
0.0159848
0.0161196
0.0131439
0.0104787
0.00909549
0.00869624
0.00879344
0.00897948
0.00813227
```

```

0.0066361
0.00584271
0.00517821
0.00460194
0.00428847
0.00403312
0.00381946
0.00363772
0.00348166
0.00334695
0.00323049
0.00313015
0.00304443
0.00297238
0.0029136
0.0028682
0.00283675
0.00282038
0.00282092
0.00284108
0.00288486
0.00295789
0.00306801
0.00322603
0.00344686
0.0037505
0.00415931
0.00468435
0.00529773
0.00590247
0.00601231
];
fid = fopen('flocculator_profiles_input.xy','w');
fprintf(fid,'((profile point %d)\n(x \n',N_out);
fprintf(fid,'%6.2f',x_h_out);
fprintf(fid,' )\n(y\n');
fprintf(fid,'%8.4f',y_h_out);
fprintf(fid,' )\n(U\n');
fprintf(fid,'%8.4f',U_out);
fprintf(fid,' )\n(tke\n');
fprintf(fid,'%14.6e',tke_out);
fprintf(fid,' )\n(epsilon\n');
fprintf(fid,'%14.6e',eps_out);
fprintf(fid,' )\n) ');
fclose(fid);

% fprintf('((profile point %d)\n(x \n',N_out);
% fprintf('%6.2f',x_h_out);
% fprintf(' )\n(y\n');
% fprintf('%8.4f',y_h_out);
% fprintf(' )\n(U\n');
% fprintf('%8.4f',U_out);
% fprintf(' )\n(tke\n');

```